Chemokine receptors CCR2 and CX3CR1 regulate viral encephalitis-induced hippocampal damage but not seizures

Christopher Käufer[a,1], Chintan Chhatbar[b,1], Sonja Bröer[a,1,2], Inken Waltl[a], Luca Ghita[b], Ingo Gerhauser[c], Ulrich Kalinke[b,d], and Wolfgang Löscher[a,d,3]

[a]Department of Pharmacology, Toxicology, and Pharmacy, University of Veterinary Medicine Hannover, 30559 Hannover, Germany; [b]Institute for Experimental Infection Research, TWINCORE, Centre for Experimental and Clinical Infection Research, a joint venture between the Helmholtz Centre for Infection Research, 38124 Braunschweig, Germany, and the Hannover Medical School, 30625 Hannover, Germany; [c]Department of Pathology, University of Veterinary Medicine Hannover, 30559 Hannover, Germany; and [d]Center for Systems Neuroscience, 30559 Hannover, Germany

Edited by Lawrence Steinman, Stanford University School of Medicine, Stanford, CA, and approved August 7, 2018 (received for review April 20, 2018)

Viral encephalitis is a major risk factor for the development of seizures, epilepsy, and hippocampal damage with associated cognitive impairment, markedly reducing quality of life in survivors. The mechanisms underlying seizures and hippocampal neurodegeneration developing during and after viral encephalitis are only incompletely understood, hampering the development of preventive treatments. Recent findings suggest that brain invasion of blood-born monocytes may be critically involved in both seizures and brain damage in response to encephalitis, whereas the relative role of microglia, the brain's resident immune cells, in these processes is not clear. CCR2 and CX3CR1 are two chemokine receptors that regulate the responses of myeloid cells, such as monocytes and microglia, during inflammation. We used *Ccr2*-KO and *Cx3cr1*-KO mice to understand the role of these receptors in viral encephalitis-associated seizures and neurodegeneration, using the Theiler's virus model of encephalitis in C57BL/6 mice. Our results show that CCR2 as well as CX3CR1 plays a key role in the accumulation of myeloid cells in the CNS and activation of hippocampal myeloid cells upon infection. Furthermore, by using *Cx3cr1*-cre$^{ER+/-}$*tdTomato*$^{St/Wt}$ reporter mice, we show that, with regard to CD45 and CD11b expression, some microglia become indistinguishable from monocytes during CNS infection. Interestingly, the lack of CCR2 or CX3CR1 receptors was associated with almost complete prevention of hippocampal damage but did not prevent seizure development after viral CNS infection. These data are compatible with the hypothesis that CNS inflammatory mechanism(s) other than the infiltrating myeloid cells trigger the development of seizures during viral encephalitis.

myeloid cells | epilepsy | Theiler's virus | hippocampus | monocytes

Temporal lobe epilepsy (TLE), the most frequent type of epilepsy in humans, is a common consequence of diverse brain insults, including traumatic brain injury, stroke, and infections of the brain (1). Common to these different acute brain injuries is the generation of an inflammatory response, which is thought to critically contribute to the development of early (insult-associated) and late (spontaneous) seizures and neurodegeneration (1). A key common brain response to injury is the rapid activation of microglia, CNS-resident innate immune cells, which promptly release inflammatory molecules including damage-associated molecular patterns, cytokines, and chemokines as well as related effector pathways including cyclooxygenase-2 and complement factors (2, 3). Furthermore, there is increasing evidence that inflammatory monocytes invading from the periphery contribute significantly to neuroinflammation and its devastating consequences after brain injury (4). However, the relative roles of invading monocytes and microglia for the short- and long-term consequences of acute brain injury are only incompletely understood.

Monocytes, i.e., mononuclear phagocytes circulating in the blood, normally do not invade the brain because of the blood–brain barrier (BBB) (5). On the basis of their differential expression of the chemokine receptors CCR2 and CX3CR1 in mice, so-called "inflammatory" (or "classic") monocytes (LY6C^{high}CCR2^{+}CX3CR1^{low}), which are highly mobile and rapidly recruited to inflamed tissues, can be distinguished from patrolling (nonclassic) monocytes (LY6C^{low}CCR2^{-}CX3CR1^{high}), which are larger in size and patrol along vascular endothelium such as the BBB (4, 6). Brain injury is typically associated with invasion of monocytes and other immune cells and concomitant amplification of local inflammation (4). Brain-resident cells produce the myelo-attractant cytokine CCL2 (also known as "monocyte chemoattractant protein 1"), a CCR2 ligand that promotes transmigration of CCR2^{+} monocytes across the BBB via CCL2/CCR2 crosstalk (7–9). Mice devoid of the *Ccr2* gene exhibit markedly reduced recruitment of monocytes and reduced pathology in several brain disease models, including autoimmune encephalitis, multiple sclerosis, stroke, and status epilepticus (9–11).

Viral encephalitis is a frequent cause of early seizures, hippocampal damage, and TLE, but the pathogenesis, mechanisms of seizures, and hippocampal neurodegeneration after encephalitis

Significance

Viral encephalitis is a frequent medical emergency, often resulting in acute seizures and brain damage, which reduce quality of life, promote the development of epilepsy, and can cause death. The relative roles of activation of microglia, the brain-resident innate immune cells, versus invasion of blood-borne immune cells such as monocytes in the acute and chronic consequences of viral encephalitis are only incompletely understood. Here we show that lack of the chemokine receptors CCR2 or CX3CR1, which regulate the responses of myeloid cells such as monocytes and microglia, prevents hippocampal damage but not seizures in a mouse model of viral encephalitis. Treatment strategies aimed at inhibiting peripheral immune cells from entering the brain during encephalitis could reduce brain damage.

Author contributions: C.K., C.C., S.B., U.K., and W.L. designed research; C.K., C.C., I.W., L.G., and I.G. performed research; C.K., C.C., I.W., L.G., U.K., and W.L. analyzed data; and C.K., C.C., U.K., and W.L. wrote the paper.

The authors declare no conflict of interest.

This article is a PNAS Direct Submission.

[1]C.K., C.C., and S.B. contributed equally to this work.

[2]Present address: Neurona Therapeutics, South San Francisco, CA 94080.

[3]To whom correspondence should be addressed. Email: wolfgang.loescher@tiho-hannover.de.

This article contains supporting information online at www.pnas.org/lookup/suppl/doi:10.1073/pnas.1806754115/-/DCSupplemental.

Published online September 4, 2018.

are only poorly understood (3). In a mouse model of viral encephalitis-induced seizures and hippocampal damage, using intracerebral inoculation of Theiler's virus [also termed "Theiler's murine encephalomyelitis virus" (TMEV)] in C57BL/6J (B6) WT mice, two groups independently reported that brain-infiltrating inflammatory monocytes damage the hippocampus (12, 13) and are key to the development of acute seizures (14). However, the experimental methods used to analyze and reduce monocyte invasion were not specific, so a role of other immune cells could not be excluded. Using a more selective approach for inhibiting monocyte invasion, i.e., administration of clodronate liposomes, we did not observe any prevention of hippocampal damage in this viral encephalitis model (15). Interestingly, in another mouse strain (SJL), in which infection with TMEV induces severe spinal cord demyelination, the use of *Ccr2*-KO mice reduced monocyte infiltration, demyelination, and long-term disease severity (16).

The objectives of the present study were threefold. The first aim was to better differentiate brain-resident myeloid cells, including microglia, from invading monocytes in the TMEV encephalitis model of TLE. For this, we compared virus-induced effects in B6 WT vs. B6-based *Cx3cr1*-cre$^{ER+/-}$*tdTomato*$^{St/Wt}$ mice in which long-lived CX3CR1^{+} cells such as microglia can be distinguished from infiltrating monocytes by the expression of the RFP tdTomato (17, 18). Second, we used B6-based *Ccr2*-KO mice to evaluate how the lack of monocyte invasion impacts the consequences of infection with TMEV in B6 mice. Third, additional experiments were performed in B6-based *Cx3cr1*-KO mice to assess the role of CX3CR1 in myeloid cell activation in the CNS during TMEV infection. In the brain, the fractalkine receptor CX3CR1 is expressed primarily on brain-resident myeloid cells, including microglia, and is critical in microglia activation and neuron–microglia communication (e.g., for recruitment of microglia to injured neurons) (5). Thus, a comparison of the consequences of viral encephalitis in *Ccr2*-KO vs. *Cx3cr1*-KO mice should allow conclusions about the relative roles of infiltrating monocytes and brain-resident myeloid cells, including microglia, in this model.

Results

Lack of CCR2, but Not of CX3CR1, Leads to Reduced Accumulation of Myeloid Cells in the CNS After Intracerebral TMEV Infection. Because CCR2 is implicated in the accumulation of infiltrating monocytes in the CNS after infection (7), whereas CX3CR1 has been proposed to be involved in microglia activation and neuron–microglia communication after CNS injury (5), we aimed to address the roles of CCR2 and CX3CR1 in viral encephalitis-induced hippocampal damage and seizure development. To this end we first investigated myeloid cell accumulation in the CNS after TMEV infection of B6 WT mice and *Ccr2*-KO or *Cx3cr1*-KO mice. For this, in brief, we perfused mice, prepared and homogenized the brain, isolated immune cells following discontinuous Percoll gradient centrifugation, and immunolabeled the

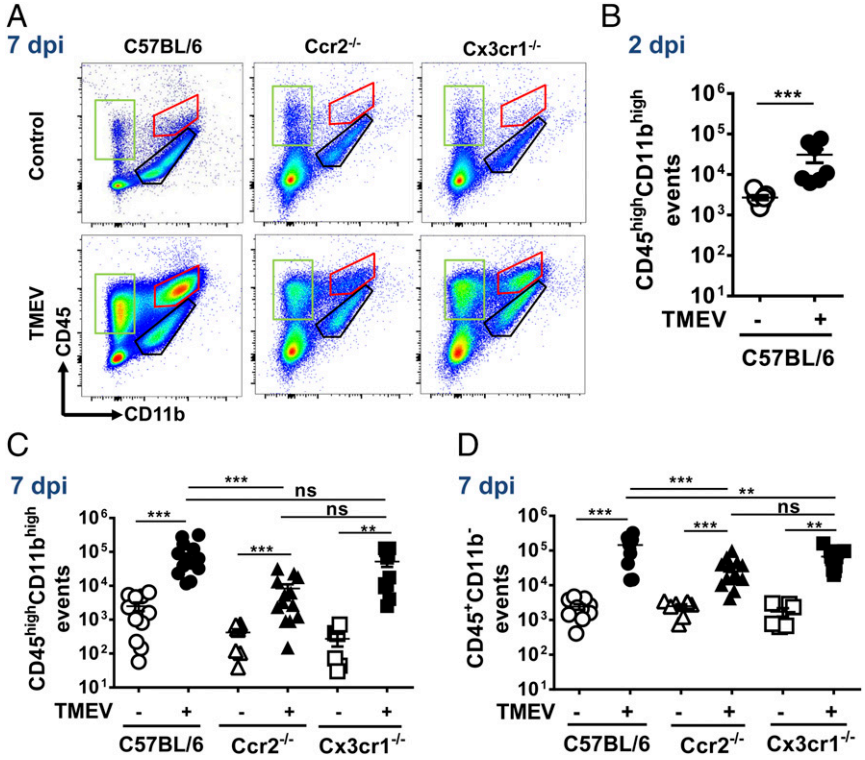

Fig. 1. Decreased accumulation of myeloid cells in the brains of CCR2-deficient but not CX3CR1-deficient mice after intracranial TMEV infection. C57BL/6 WT, *Ccr2*-KO, and *Cx3cr1*-KO animals were mock infected or infected with TMEV intracranially. Animals were killed at 2 or 7 dpi. After enzymatic digestion, immune cells were isolated using Percoll gradient and were immunolabeled, and flow cytometry was performed. Myelin debris and dead cells were excluded by FSC/SSC gating, and singlet populations were analyzed. (*A*) Representative flow cytometry data of immune cells isolated from the brains at 7 dpi. (*B*) Quantification of CD45^{high}CD11b^{high} myeloid cells in the brain at 2 dpi (red-marked population in *A*). Shown are combined data of two independent experiments; $n = 7$. (*C*) Quantification of CD45^{high}CD11^{high} myeloid cells in the brain at 7 dpi (red-marked population in *A*). Shown are combined data of two independent experiments; $n = 6$–14). (*D*) Quantification of CD45^{+}CD11b^{-} cells in the brain at 7 dpi (green-marked population in *A*). Shown are combined data of two independent experiments; $n = 6$–13). The data in *B*–*D* are shown as mean ± SEM (plus individual data). Analysis of data in *C* by two-way ANOVA indicated a significant effect of infection [F (1, 57) = 13.91; $P = 0.0004$], genotype [F (2, 57) = 3.98; $P = 0.0241$], and interaction [F (2, 57) = 3.601; $P = 0.0337$]. Similar, analysis of data in *D* indicated a significant effect of infection [F (1, 52) = 36.29; $P < 0.0001$], genotype [F (2, 52) = 7.054; $P = 0.0019$], and interaction [F (2, 52) = 7.034; $P = 0.002$]. Post hoc results in *B*–*D* are indicated by asterisks: $^{**}P < 0.01$; $^{***}P < 0.001$); ns, not significant.

cells and analyzed them cytofluometrically by first excluding myelin debris and dead cells by forward scatter versus side scatter (FSC/SSC) gating followed by subsequent gating on singlet populations (*Methods*). In accordance with previous reports (12–15), infection of B6 mice with TMEV resulted in a significant increase in the number of $CD45^{high}CD11b^{high}$ myeloid cells in the CNS at 2 and 7 d postinfection (dpi) as indicated by flow cytometry analysis of brains (Fig. 1 *A*–*C*). Since we observed particularly high accumulation of myeloid cells in the CNS at 7 dpi, we chose this time point for further analysis.

CCR2 is required for the egress of monocytes from the bone marrow to the blood as well as for migration of blood monocytes into the inflamed tissue (7, 19). TMEV infection of *Ccr2*-KO mice resulted in a significant accumulation of $CD45^{high}CD11b^{high}$ myeloid cells at 7 dpi in the CNS (Fig. 1 *A* and *C*). However, this accumulation of $CD45^{high}CD11b^{high}$ myeloid cells was significantly less than in B6 WT animals (Fig. 1 *A* and *C*). It has been shown previously that lack of CX3CR1 leads to apoptosis of $Ly6C^{low}Cx3cr1^{high}$ monocytes in the blood (20). TMEV infection of *Cx3cr1*-KO animals also resulted in a significant accumulation of $CD45^{high}CD11b^{high}$ myeloid cells at 7 dpi, which was comparable with the accumulation in B6 WT animals. Minute accumulation of immune cells was also observed in sham controls, most likely as a result of intracerebral injection of mock solution.

Both *Ccr2*-KO and *Cx3cr1*-KO animals showed significantly reduced accumulation of $CD45^{+}CD11b^{-}$ cells compared with B6 WT animals, although the difference from infected B6 WT mice was low (Fig. 1 *A* and *D*). To exclude the possibility that the minor reduction of lymphocytes in the genetically manipulated hosts led to inefficient virus clearance, we determined TMEV antigen in the whole brain and hippocampus of infected mice at 7 dpi. In B6 WT mice, the virus is cleared within 2 wk after infection, predominantly by $CD8^{+}$ cytotoxic T lymphocytes (3). As shown in *SI Appendix*, Fig. S3, there was no indication that genetically manipulated hosts cleared the virus less rapidly than infected WT mice; rather, the opposite was found.

Interestingly, unlike $CD45^{high}CD11b^{high}$ myeloid cells, $CD45^{low}CD11b^{low}$ cells (i.e., microglia) were not significantly increased in infected WT mice (*SI Appendix*, Fig. S1). However, TMEV-infected *Ccr2*-KO and *Cx3cr1*-KO mice had significantly fewer $CD45^{low}CD11b^{low}$ cells than WT mice.

Since *Ccr2*-KO animals showed reduced recruitment of $CD45^{high}CD11b^{high}$ myeloid cells in the CNS upon TMEV infection, we investigated the number of monocytes in the blood at 7 dpi. In the WT animals there was normal distribution of CSF-$1R^{+}$ monocytes in the blood (*SI Appendix*, Fig. S2). As reported previously (19, 20), we detected reduced numbers of circulating CSF-$1R^{+}$ monocytes in the blood of both *Ccr2*-KO and *Cx3cr1*-KO mice (*SI Appendix*, Fig. S2). However, CSF-$1R^{+}$ monocytes were entirely absent in *Ccr2*-KO animals, whereas in *Cx3cr1*-KO animals there was only a reduction in the number of such monocytes, which accounted for the accumulation of $CD45^{high}CD11b^{high}$ myeloid cells in the brain. In conclusion, the lack of CSF-$1R^{+}$ monocytes in *Ccr2*-KO mice leads to reduced accumulation of myeloid cells in the CNS during TMEV infection, whereas in *Cx3cr1*-KO animals the accumulation of myeloid cells is comparable to that in B6 WT animals.

CCR2 and CX3CR1 Regulate the Activation and Proliferation of Myeloid Cells in the Hippocampus After TMEV Infection. During the development of TLE after brain insults, morphological and functional alterations of the hippocampus are thought to contribute critically to the epileptogenesis and cognitive impairment often associated with TLE (1). Hippocampal sclerosis with degeneration

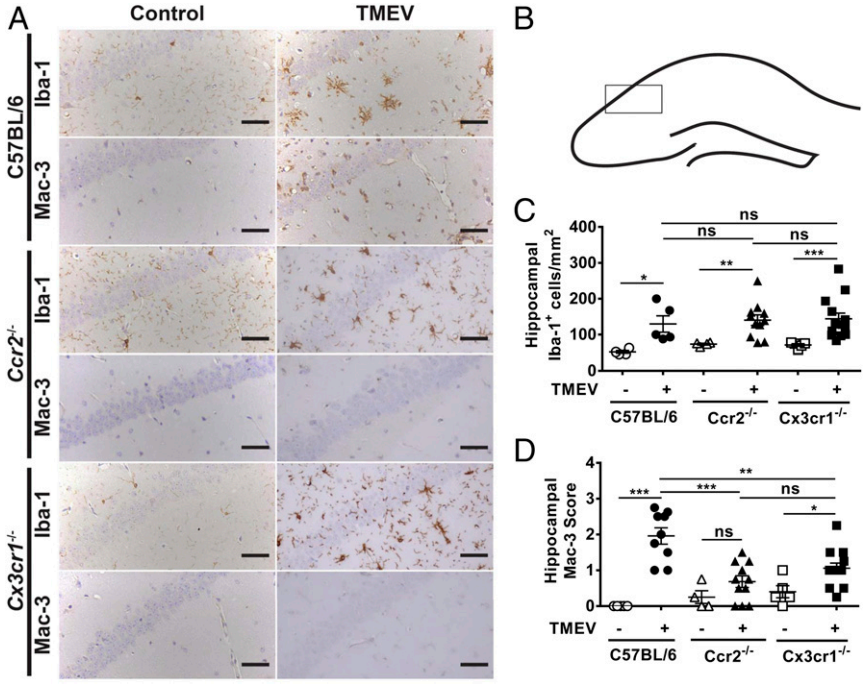

Fig. 2. Genetic deficiency of CCR2 but not CX3CR1 leads to decreased activation of myeloid cells in the hippocampus after intracranial TMEV infection. Animals were treated as described in Fig. 1. On day 7 after perfusion brains were removed, and immunohistology was performed. (*A*) Representative examples of Iba-1– and Mac-3–stained hippocampal sections. (Scale bars: 50 μm.) (*B*) Area of the hippocampus from which the sections shown in *A* were taken. (*C*) Quantification of hippocampal Iba-1^{+} cells shown in *A*. (*D*) Semiquantitative data for Mac-3 staining shown in *A*. The data in *C* and *D* are shown as mean ± SEM (plus individual data). Analysis of data in *C* by two-way ANOVA indicated a significant effect of infection [(F (1, 36) = 20.89; $P < 0.0001$] but not genotype [F (2, 36) = 0.4272; $P = 0.6556$] or interaction [F (2, 36) = 0.03501; $P = 0.9656$]. Analysis of data in *D* indicated a significant effect of infection [F (1, 41) = 38.21; $P < 0.0001$], genotype [F (2, 41) = 3.088; $P \leq 0.05$], and interaction [F (2, 41) = 8.251; $P = 0.0010$]. Post hoc results are indicated by asterisks: *$P < 0.05$; **$P < 0.01$; ***$P < 0.001$; ns, not significant.

of neurons in CA1, CA3, and the dentate hilus is the most common pathology of TLE, but the underlying mechanisms of the neuronal degeneration are only poorly understood (1). A similar type of hippocampal damage is also observed in the TMEV model of TLE in B6 mice (14, 15, 21). Since we observed a decreased accumulation of myeloid cells by flow cytometry analysis of whole brains from TMEV-infected *Ccr2*-KO animals, we next investigated the accumulation of myeloid cells in the hippocampus of infected mice by immunohistochemical analysis of the common myeloid cell marker Iba-1$^+$, which is expressed by resting and activated microglia as well as monocytes (22). Similar to the flow cytometry analysis, the histochemical analysis also revealed that TMEV-infected WT animals showed a significant accumulation of Iba-1$^+$ myeloid cells in the hippocampus compared with control animals at 7 dpi (Fig. 2 *A* and *C*). In addition to counting Iba-1$^+$ cells in the hippocampus, we also examined the shape of Iba-1$^+$ cells. In WT control animals the Iba-1$^+$ cells showed the typical microglial morphology with a small cell body and many long and thin ramifications. Upon TMEV infection of WT animals most of the Iba-1$^+$ cells showed an increased cell body volume with short thick processes, suggesting activation of microglia, whereas some cells had round or elongated shapes suggesting infiltration of monocytes from the periphery (Fig. 2*A*).

Infected *Ccr2*-KO animals showed similarly increased numbers of Iba-1$^+$ cells in the hippocampus as infected WT animals, suggesting increased accumulation of myeloid cells in the hippocampus in infected *Ccr2*-KO mice (Fig. 2 *A* and *C*). The shape of the Iba-1$^+$ cells suggested that activated microglia similar to those observed in infected WT controls were present in several mice (Fig. 2*A*). Similarly, *Cx3cr1*-KO animals showed a significant increase in the number of Iba-1$^+$ cells in the hippocampus of TMEV-infected animals compared with noninfected *Cx3cr1*-KO animals (Fig. 2 *A* and *C*), and the shape of the Iba-1$^+$ cells suggested that activated microglia were present in several mice (Fig. 2*A*). Comparison of the accumulation of Iba-1$^+$ myeloid cells in infected WT, *Ccr2*-KO, and *Cx3cr1*-KO mice showed that there was no significant difference in the accumulation of myeloid cells within the hippocampus among these three groups of animals upon TMEV infection (Fig. 2*C*). This, however, did not allow any conclusions about differences in the type of myeloid cells (resting vs. activated vs. proliferating microglia vs. monocytes) across genotypes.

Activated myeloid cells release many proinflammatory mediators which damage neurons and cause their death (21). We analyzed the activation of Iba-1$^+$ myeloid cells by analyzing hippocampal expression of Mac-3, which, like Iba-1, is expressed by activated microglia as well as monocytes (23). This analysis showed that myeloid cells from noninfected WT control animals did not express Mac-3, suggesting that these cells were not activated, whereas TMEV infection of WT animals led to a high expression of Mac-3 in the hippocampus, indicating that the myeloid cells were activated after infection (Fig. 2 *A* and *D*). In the *Ccr2*-KO or *Cx3cr1*-KO animals we observed a low expression of Mac-3 in the hippocampus of control animals, suggesting mild activation of myeloid cells. Mac-3 expression did not increase significantly upon TMEV infection in *Ccr2*-KO animals ($P = 0.1934$), but a significant increase was observed in *Cx3cr1*-KO animals (Fig. 2 *A* and *D*). However, compared with infected B6 WT mice, the increase in Mac-3–labeled cells in infected *Cx3cr1*-KO mice was significantly less marked (Fig. 2*D*).

In response to a variety of CNS insults such as microbial invasion, resting microglia have the capacity to dramatically change their morphology into an activated phenotype (24). However, microglia activation can also be the consequence of the proliferation of microglia, as previously shown in B6 mice infected with TMEV (25). We therefore examined whether microglia proliferation is altered by *Ccr2* KO or *Cx3cr1* KO, using colabeling for Ki67 and Iba-1. As shown in Fig. 3 *A* and *C*, in noninfected controls of either genotype almost no Ki67/Iba-1 double-labeled cells were observed, whereas a significant increase in Ki67/Iba-1 double-labeled cells was determined in the hippocampus of infected WT mice. Thirteen to sixty-seven percent (mean 36%) of the Iba-1$^+$ cells were also labeled by Ki67 in infected WT mice (Fig. 3*D*). In contrast, microglia proliferation was suppressed in both Ccr2-KO and Cx3cr1-KO mice (Fig. 3 *A*, *C*, and *D*).

Activated Myeloid Cells Present in the CNS After TMEV Infection Consist of Microglia and Infiltrating Monocytes. Based on flow cytometry analysis of CD45 and CD11b, previous studies have reported the accumulation of infiltrating monocytes in the CNS during TMEV infection (12–15). However, recent studies have shown that during neuroinflammation microglia up-regulate CD45 expression and become indistinguishable from monocytes (22, 26, 27), so the specific function of invading monocytes has been difficult to address (4). To differentiate infiltrating monocytes from CNS-resident myeloid cells such as microglia, we used *Cx3cr1-cre*$^{ER+/-}$*tdTomato*$^{St/Wt}$ reporter mice carrying a tamoxifen-inducible cre^{ER} and a cre-inducible tdTomato reporter. In these mice CX3CR1$^+$ myeloid cells, such as microglia and circulating monocytes, are marked by expression of the tdTomato reporter upon tamoxifen injection. Due to replenishment of all recirculating tdTomato-expressing CX3CR1$^+$ cells (such as monocytes) by tdTomato$^-$ cells within 8 wk following the tamoxifen treatment, this approach allows the discrimination of long-lived CX3CR1$^+$ cells, such as microglia, from peripheral monocytes (17, 18).

In the first step, by flow cytometry analyses we ensured that the genetic marking of myeloid cells did not alter the accumulation of immune cells in the CNS after TMEV infection. Indeed, upon TMEV infection 8 wk after tamoxifen treatment, we observed myeloid cell accumulation in the brains of these mice that was comparable with that in WT animals (Fig. 4 *A* and *D*; see Fig. 1 for WT). Next, we used tdTomato expression to distinguish microglia from infiltrating monocytes by flow cytometry. In the CD45^{low}CD11b^{low} population most of the cells expressed the tdTomato reporter (Fig. 4*B*), showing high targeting of microglia as reported previously (17). Since we wanted to investigate whether some of the CD45^{low} microglia up-regulated CD45 and became CD45^{high} upon TMEV infection, we compared the number of tdTomato$^+$ cells in the CD45^{high}CD11b^{high} populations in control and TMEV-infected animals. This analysis showed that there was a significant increase in the number of tdTomato$^+$ cells within the CD45^{high}CD11b^{high} population in TMEV-infected animals compared with control animals (Fig. 4 *B* and *E*). In the *Cx3cr1-cre*$^{ER+/-}$*tdTomato*$^{St/Wt}$ mice, tamoxifen treatment also leads to the expression of the tdTomato reporter in CNS vessel-associated myeloid cells such as perivascular macrophages and meningeal macrophages, and these cells are also long-lived (18). These cells express high levels of CD45 as well as the mannose receptor CD206, whereas microglia typically do not express CD206 (28). Therefore, to differentiate between CD45^{high} microglia and the vessel-associated macrophages present within the CD45^{high}CD11b^{high}tdTomato$^+$ population from infected mice, we analyzed the expression of CD86 and CD206 on these cells. In noninfected control animals as well as in TMEV-infected animals we detected more than 90% cells within the CD45^{high}CD11b^{high}tdTomato$^+$ population that did not express CD206 and very few cells expressing CD206 (Fig. 4*C*). Expression of CD86 on these cells confirmed that these cells were activated (Fig. 4*C*). This analysis showed that upon TMEV infection of the CNS most, if not all, of the CD45^{high}CD11b^{high}tdTomato+ cells were microglia and not CNS vessel-associated macrophages. We further confirmed infiltration of peripheral monocytes in the CNS by the analysis of the number of tdTomato$^-$ cells within the CD45^{high}CD11b^{high} population, which significantly increased

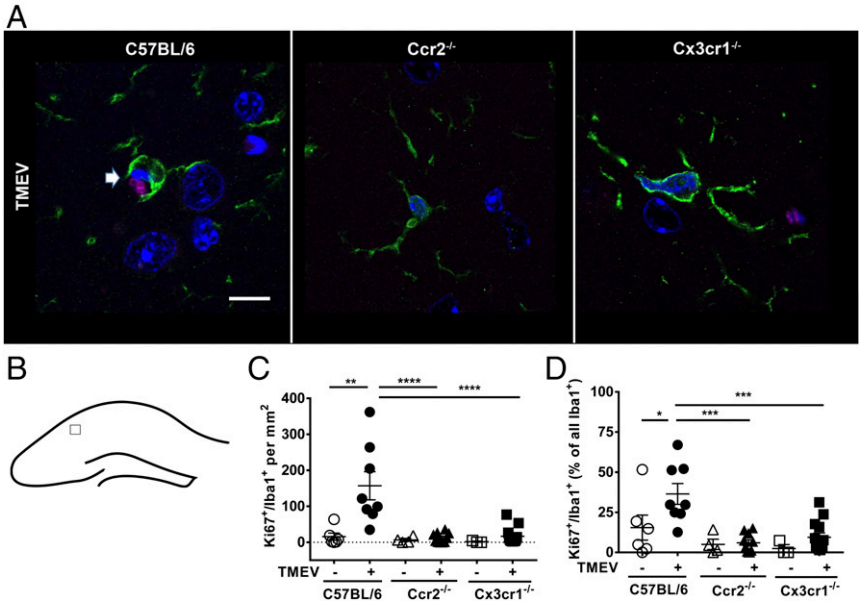

Fig. 3. Genetic deficiency of CCR2 and CX3CR1 prevents microglia proliferation in the hippocampus after intracranial TMEV infection. Animals were treated as described in Fig. 1; on day 7 after perfusion, brains were removed, and immunohistology was performed. (*A*) Representative examples of Iba-1 and Ki67 double-stained cells in hippocampal sections. Slice thickness was only 2 μm (*Methods*), so processes of Iba-1$^+$ microglial cells (green) are often cut from the cell bodies. Cell nuclei were stained using DAPI (blue); Ki67$^+$ is shown in magenta. A Iba-1$^+$/Ki67$^+$ microglial cell (arrow) can be seen in this example of an infected B6 WT mouse, while Iba-1$^+$ cells in *Ccr2*-KO and *Cx3cr1*-KO mice are mainly negative for Ki67 (see also *C*). (Scale bar: 10 μm.) (*B*) Area of the hippocampus from which the sections shown in *A* were taken. (*C*) Quantification of Iba-1$^+$/Ki67$^+$ double-labeled cells shown in *A* in the ipsilateral hippocampus. (*D*) Percent of Iba-1$^+$ cells that are also positive for Ki67 (proliferation index). The data in *C* and *D* are shown as mean ± SEM (plus individual data). Analysis of data in *C* by two-way ANOVA indicated a significant effect of infection [F (1, 38) = 9.88; P = 0.0032], genotype [F (2, 38) = 9.664; P = 0.0004], and interaction [F (2, 38) = 7.038; P = 0.0025]. Analysis of data in *D* indicated a significant effect of infection [F (1, 38) = 5.243; P = 0.0277] and genotype [F (2, 38) = 11.2; P = 0.0002] but not interaction [F (2, 38) = 2.186; P = 0.1263]. Post hoc results are indicated by asterisks: *P < 0.05; **P < 0.01; ***P < 0.001; ****P < 0.0001.

upon infection (Fig. 4 *B* and *F*). In conclusion, upon TMEV infection a population of microglia up-regulates CD45 expression and by CD45 and CD11b expression becomes indistinguishable from infiltrating monocytes.

CCR2 and CX3CR1 Are Involved in Hippocampal Neurodegeneration After TMEV Encephalitis. As reported previously (21), TMEV-induced encephalitis in B6 WT mice was predominantly associated with damage in the hippocampus as a result of the virus tropism to this region in this mouse strain. Within the hippocampus, the CA1 and CA2 pyramidal cell layers were severely damaged, as indicated by the decrease in NeuN staining (Fig. 5 *A* and *B*). No such damage was observed in NeuN-immunostained sections from infected *Ccr2*-KO or *Cx3cr1*-KO mice (Fig. 5 *A* and *B*). For further analysis of neurodegeneration in the hippocampus, sections were stained with Fluoro-Jade C (FJC), a sensitive and specific fluorescent marker of dying neurons (29). In mock-infected controls, no FJC-stained neurons were detected, while intense staining of pyramidal cells was observed in the CA1 and CA2 layers of several TMEV-infected WT animals (Fig. 5 *C* and *D*). In *Ccr2*-KO mice, no FJC-labeled cells were observed, whereas a few FJC-labeled cells were detected in *Cx3cr1*-KO mice (Fig. 5 *C* and *D*). In conclusion, CCR2 and CX3CR1 play a key role in hippocampal neurodegeneration during TMEV encephalitis.

Neither *Ccr2* nor *Cx3cr1* Knockout Prevents Acute Seizures in TMEV-Infected Mice, but Lack of CCR2 Reduces Seizure Severity. Since hippocampal damage is frequently associated with seizure development in animal models and patients with acquired partial epilepsy (1), we hypothesized that decreased hippocampal neurodegeneration could lead to a decrease in TMEV encephalitis-induced seizure development. To address this question, we monitored seizure development in TMEV-infected WT, *Ccr2*-KO, and *Cx3cr1*-KO animals. The temporal (bell-shaped) profile of seizure incidence over the 7 d after infection did not differ among groups (Fig. 6*A*); in all three groups maximum seizure incidence occurred at 2 dpi. Cumulative seizure incidence was 67% in infected WT mice, 54% in infected *Ccr2*-KO mice, and 69% in infected *Cx3cr1*-KO mice, without significant intergroup differences (Fig. 6*B*). Similarly, seizures were observed in 82% of *Cx3cr1-cre*$^{ER+/-}$*tdTomato*$^{St/Wt}$ animals. Mock-infected WT and mock-infected *Ccr2*-KO, *Cx3cr1*-KO, or *Cx3cr1-cre*$^{ER+/-}$*tdTomato*$^{St/Wt}$ animals did not exhibit any seizures.

Raw Racine scores (30) recorded for each animal indicated that seizure severity was significantly lower in *Ccr2*-KO mice than in WT or *Cx3cr1*-KO mice, due to a change in the number of low (stage 3) Racine events vs. high (stage 4/5) Racine events in the Ccr2-KO mice (Fig. 6*C*). Similarly, when average seizure severity was calculated per mouse with seizures, seizure severity was significantly lower in *Ccr2*-KO mice (3.207 ± 0.0955) than in B6 WT mice (3.808 ± 0.1897; P = 0.0403) and *Cx3cr1*-KO mice (3.887 ± 0.1647; P = 0.0029).

The number of observed seizures (i.e., seizure frequency) did not differ among the groups (Fig. 6*D*). Furthermore, the cumulative seizure burden was similar in all groups (Fig. 6*E*). In conclusion, CCR2 and CX3CR1 do not regulate seizure development following TMEV encephalitis, but CCR2 seems to be involved in seizure severity.

Discussion

Recent studies indicated that brain infiltration with inflammatory monocytes plays a major role in the pathological consequences of viral encephalitis in B6 mice, a widely used model of TLE (21). While some neuronal loss during viral encephalitis may result from direct virus-mediated injury, much of the damage is associated with bystander pathology as a result of activation of the innate

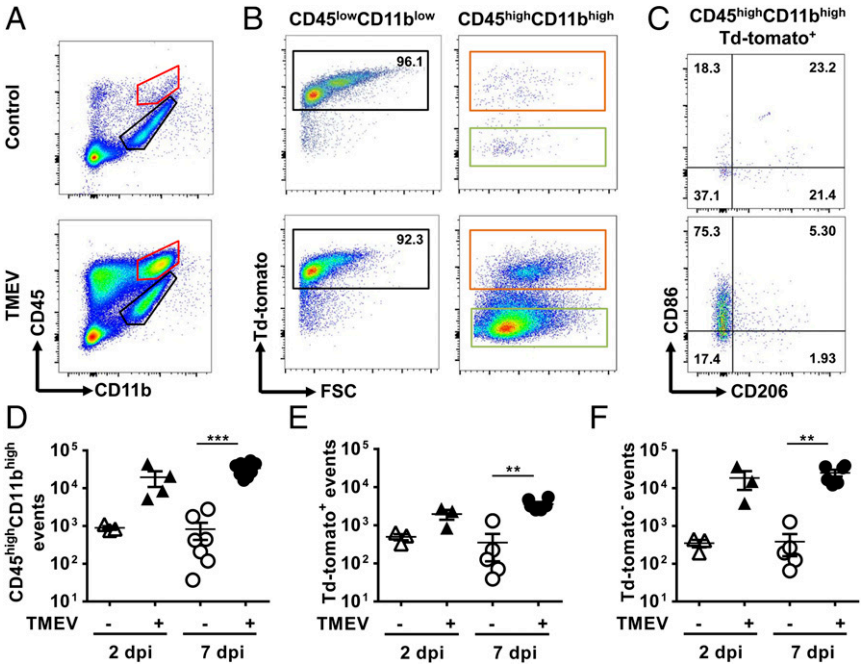

Fig. 4. A population of microglia up-regulates CD45 and becomes indistinguishable from infiltrating monocytes after intracranial TMEV infection. Tamoxifen-treated *Cx3cr1-cre*$^{ER+/-}$*tdTomato*$^{St/Wt}$ mice were infected, and CNS immune cells were isolated as described in Fig. 1. (*A*) Representative flow cytometry data of immune cells isolated from brain. (*B*) Representative flow cytometry data of tdTomato expression on CD45^{low}CD11b^{low} cells (black-marked population in *A*) and CD45^{high}CD11b^{high} cells (red-marked population in *A*). (*C*) Expression of CD86 and CD206 on the CD45^{high}CD11b^{high}tdTomato^{+} cells (orange-marked population in *B*). (*D*) Quantification of CD45^{high}CD11^{high} myeloid cells in the brain at 2 and 7 dpi (red-marked population in *A*). Shown are the combined data of two independent experiments; $n = 3–8$. (*E*) Quantification of tdTomato-expressing cells in the CD45^{high}CD11b^{high} population in *A* (orange-marked population in *B*); $n = 3–6$; shown are combined data of two independent experiments. (*F*) Quantification of tdTomato^{-} cells in the CD45^{high}CD11b^{high} population in *A* (green-marked population in *B*; $n = 3–6$; combined data from two independent experiments are shown). The data in *D–F* are shown as mean ± SEM (plus individual data); open symbols represent mock-infected controls, filled symbols represent infected mice. Analysis of data in *D* by two-way ANOVA indicated a significant effect of infection [F (1, 18) = 25.23; $P < 0.0001$] but not time [F (1, 18) = 1.891; $P = 0.1859$] or interaction [F (1, 18) = 1.931; $P = 0.1816$]. Similar, analysis of data in *E* and *F* indicated only a significant effect of infection [*E*: F (1, 13) = 27.66; $P = 0.0002$; *F*: F (1, 13) = 17.58; $P = 0.0011$]. Post hoc results are indicated by asterisks: $^{**}P < 0.01$; $^{***}P < 0.001$.

immune system (12, 13, 31). The same is true for the insult-associated seizures observed in the first week after infection (32). Inflammatory monocytes can secrete proinflammatory cytokines such as IL-6, IL-1β, and TNF-α, which have been implicated in the development of acute seizures and hippocampal damage in the TMEV model of encephalitis (21). Furthermore, activation of the calcium-dependent cysteine protease calpain in hippocampal neurons seems to be involved in viral encephalitis-induced neurodegeneration (31, 33). However, neuroinflammation is generally a collaborative interaction between brain-resident cells such as microglia and astrocytes and infiltrating cells such as inflammatory monocytes, neutrophils, and other leukocytes. Therefore, it is highly unlikely that encephalitis-induced pathology is a result of monocyte invasion alone. Indeed, a marked activation of microglia has been determined in the hippocampus of TMEV-infected B6 mice (25, 34). Once the innate immune response is triggered, secretion of proinflammatory chemokines and cytokines contributes to the induction of the adaptive immune response by recruiting immune cells, such as T lymphocytes, to the site of infection, resulting in virus clearance (35). However, in contrast to innate immunity, the adaptive immune system seems not to be critically involved in hippocampal damage and early seizures in the TMEV model of TLE (21, 35). In the present study we examined the roles of CCR2 and CX3CR1, two important chemokine receptors expressed by myeloid cells such as microglia and monocytes, in TMEV CNS infection-induced seizure development, using the Daniel's (DA) strain of TMEV. Further, we used *Cx3cr1-cre*$^{ER+/-}$*tdTomato*$^{St/Wt}$ mice to differentiate between long-lived CNS-resident myeloid cells such as microglia and infiltrating peripheral monocytes during TMEV CNS infection. Several surprising findings were obtained that significantly change the current understanding of viral encephalitis-induced brain pathology.

In accordance with the previously published literature, our experiments in *Cx3cr1-cre*$^{ER+/-}$*tdTomato*$^{St/Wt}$ mice substantiated the massive monocyte infiltration in the brain of TMEV-infected mice. In previous studies the accumulation of myeloid cells in the CNS and hippocampus was shown to be associated with hippocampal neurodegeneration and the development of seizures (12–15, 21). Lack of CCR2 but not CX3CR1 markedly reduced the accumulation of the myeloid cells in the brains of TMEV-infected mice, which could be explained by the lack of circulating monocytes in the blood of *Ccr2*-KO mice (19). One of the key problems associated with studies using WT mice is the inability to differentiate between different types of myeloid cells in the CNS, particularly under CNS inflammation. It is known that under CNS inflammation microglia can up-regulate the expression of CD45, which is commonly used to distinguish between microglia and other myeloid cells in the CNS during steady-state conditions (22). Previous studies used LysM-GFP reporter mice or bone marrow chimera to address the phenomenon of CD45 up-regulation of microglia during TMEV CNS infection (13, 14). However, because in these studies monocytes and neutrophils were marked by GFP expression, it was not possible to selectively identify microglia, which might have been present in the CD45^{high} population. Thus, these studies could only conclude that there was infiltration of monocytes from periphery upon TMEV CNS infection (13, 14), so the possibility of microglia up-regulating CD45 expression has not yet been addressed in this

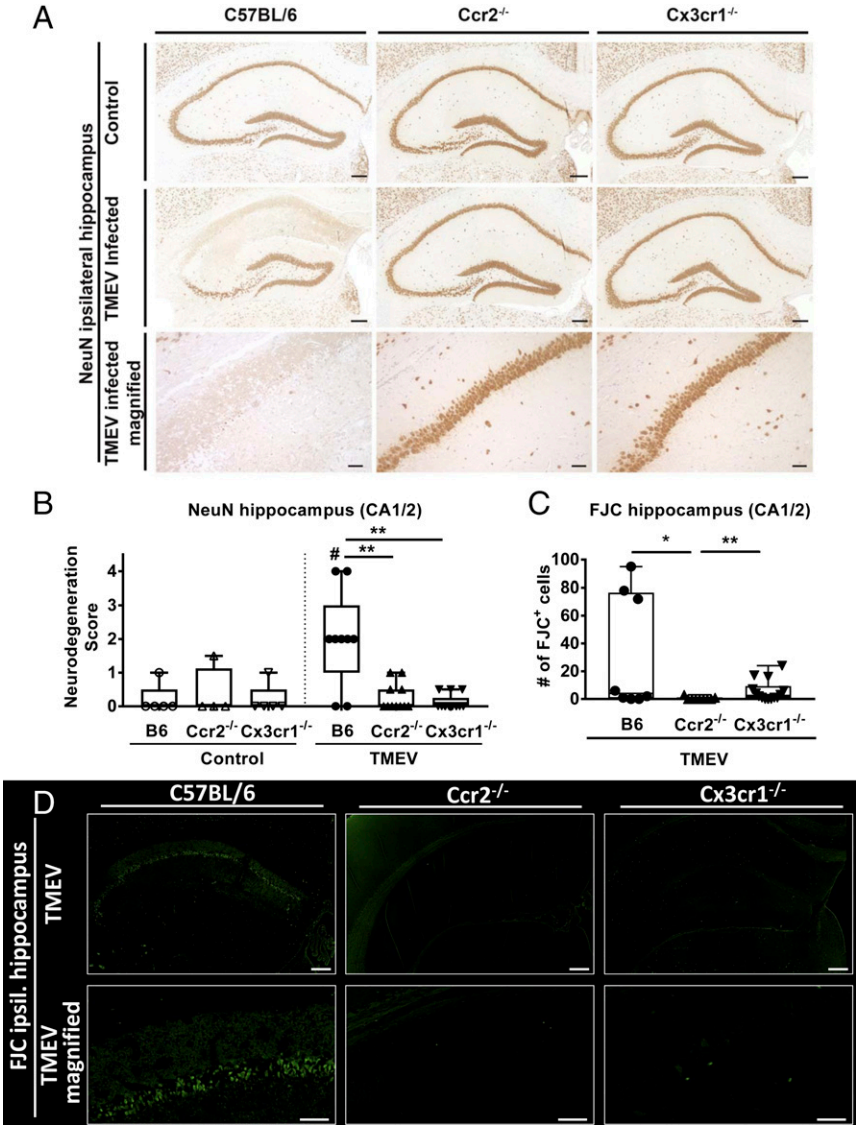

Fig. 5. Genetic deficiency of CCR2 and CX3CR1 leads to decreased neuronal death in the hippocampus after TMEV infection. Animals were treated as described in Fig. 1. Brains were removed on day 7 after perfusion, and histology was performed on sections of the dorsal hippocampus. Section levels (−2.06 ± 0.26 mm from bregma) were similar in all groups. (*A*) Representative photomicrographs illustrating NeuN$^+$ neurons in mock-infected and TMEV-infected B6, *Ccr2*-KO, and *Cx3cr1*-KO mice. [Scale bars: 200 μm (overview, *Top* and *Center Rows*) or 50 μm (magnification, *Bottom Row*).] (*B*) Semi-quantitative data on NeuN$^+$ neurons in the CA1/CA2 regions of the hippocampus. Data are shown as boxplots with whiskers indicating minimum and maximum values; the horizontal line in the boxes represents the median value. In addition, individual data are shown (n = 5–13). Analysis of data by two-way ANOVA indicated a significant effect of infection [F (1, 41) = 5.33; P = 0.0261], genotype [F (2, 41) = 6.348; P = 0.0040], and interaction [F (2, 41) = 7.35; P = 0.0019]. Significant differences from post hoc testing of mock-infected mice are indicated by the hash sign: $^{\#}P < 0.05$; significant differences between infected groups are indicated by asterisks: $^{**}P < 0.01$. (*C*) The number of FJC$^+$ neurons in infected mice (n = 6–14). No FJC staining was observed in controls. Analysis of data by one-way ANOVA indicated a significant difference between groups [F (2, 28) = 5.174; P = 0.0122]. Significant differences between infected groups are indicated by asterisks: $^{*}P < 0.05$; $^{**}P < 0.01$. (*D*) Representative photomicrographs illustrating FJC staining in infected mice. [Scale bars: 200 μm (*Top Row*) or 50 μm (*Bottom Row*).]

model. Using *Cx3cr1-cre*$^{ER+/-}$*tdTomato*$^{St/Wt}$ mice, we show here that during viral encephalitis a population of microglia upregulates CD45 and thus become indistinguishable from infiltrating monocytes. Therefore, the conclusions from previous studies (12–15, 21), which relied on CD45 and CD11b expression to differentiate microglia from infiltrating CD45^{high} monocytes under conditions of viral encephalitis in the TMEV model, need to be reevaluated.

Since inflammatory response is the final effector mechanism of hippocampal neurodegeneration and seizures, we next focused on assessing the impact of CCR2 and CX3CR1 on CNS inflammation. As myeloid cells have been implicated in hippocampal damage and epilepsy (12–15, 21), we decided to assess the activation of myeloid cells present in the hippocampus of TMEV-infected animals. Determination of virus antigen demonstrated that neither *Ccr2*-KO nor *Cx3cr1*-KO retarded virus clearance in the brain. Staining of the myeloid cell-activation marker Mac-3 revealed that TMEV-infected WT mice showed high activation of myeloid cells in the hippocampus, whereas knock out of *Ccr2* or *Cx3cr1* resulted in decreased infection-dependent activation. One of the reasons for the decrease in Mac-3 expression could be the decreased accumulation of myeloid cells in the hippocampus. Although we observed decreased accumulation of myeloid cells in the flow cytometry analysis of whole brains of *Ccr2*-KO animals upon infection, Iba-1 immunostaining for myeloid cells showed that there was similar accumulation of Iba-1$^+$ myeloid cells in the hippocampus upon TMEV infection, independent of genotype of the animals, suggesting that the decrease in Mac-3 staining was indeed due to reduced activation of myeloid cells. Double-labeling of proliferating cells with Ki67 and Iba-1 substantiated increased proliferation of microglia in the hippocampus of infected WT mice, as previously reported (25), but this was suppressed in both Ccr2-KO and Cx3cr1-KO mice. These data show that both CCR2 and CX3CR1 play a role in the activation and proliferation of myeloid cells in the CNS during viral encephalitis-induced neurodegeneration and epilepsy.

The reduced activation and proliferation of myeloid cells in the hippocampus of infected *Ccr2*-KO and *Cx3cr1*-KO mice motivated us to investigate their impact on hippocampal neurons, as hippocampal damage is associated with the development of seizures and epilepsy following different brain insults, including viral encephalitis (1), although neuronal degeneration is not always a prerequisite for generation of seizures (36). NeuN and FJC staining of the hippocampus showed that TMEV infection in WT animals can lead to heavy loss of neurons in the

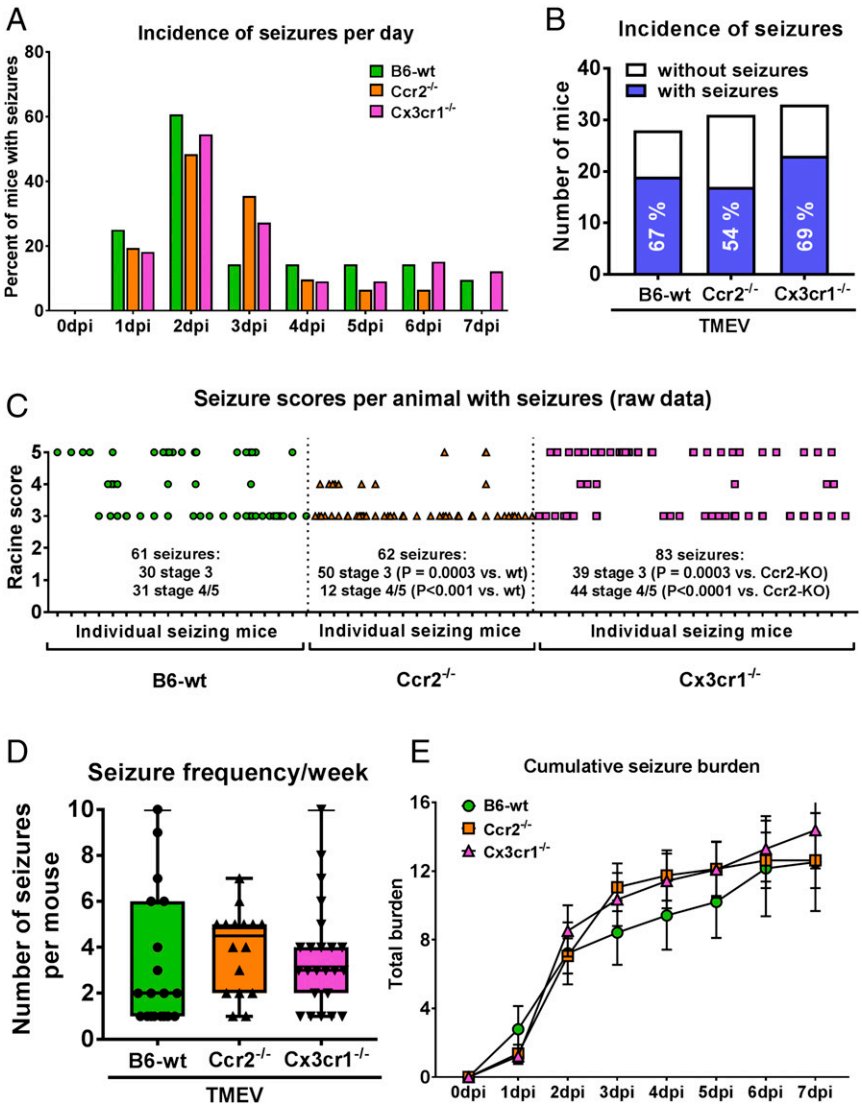

Fig. 6. Genetic deficiency of CCR2 and CX3CR1 does not decrease seizure incidence after TMEV infection. Mice were treated as described in Fig. 1, and the incidence, frequency, and severity of seizures were calculated over the 7-d monitoring period. Group sizes were 28 B6-WT, 31 *Ccr2*-KO, and 33 *Cx3cr1*-KO mice. (*A*) Temporal profile of seizure incidence following infection; analysis of data by Fisher's exact test did not indicate significant intergroup differences. (*B*) Cumulative seizure incidence calculated from the data shown in *A*. Seizure incidence is indicated by the blue part of the columns; exact percentages are indicated within the columns. No seizures were observed in mock-infected controls (not shown; $n = 28–33$); analysis of data by Fisher's exact test did not indicate significant intergroup differences. (*C*) Raw Racine scores for each seizure in each animal recorded over the 7 d following infection. Each tick mark on the *x* axis represents a mouse with observed seizure(s); each symbol represents a single seizure. *Ccr2*-KO mice exhibited significantly fewer generalized convulsive (stage 5) seizures than B6-WT ($P < 0.05$) or *Cx3cr1*-KO mice ($P < 0.01$; Fisher's exact test). (*D*) The number of seizures counted in each mouse, i.e., seizure frequency recorded over the 7 dpi. Data are shown as boxplots with whiskers indicating minimum and maximum values; the horizontal lines in the boxes represent the median value. In addition, individual data are shown. Analysis of data by ANOVA did not indicate significant differences ($P = 0.7178$). (*E*) Cumulative seizure burden at each day postinfection in the three groups of mice. Cumulative seizure burden at each day postinfection for a mouse was calculated by summing all its seizure scores up to that day. No significant intergroup differences were observed.

CA1 and CA2 sectors, whereas neuronal loss was prevented in the *Ccr2*-KO and *Cx3cr1*-KO animals. These data show that during viral encephalitis-induced brain pathology hippocampal inflammation and neurodegeneration can be regulated by modulating CCR2 and CX3CR1. The observed suppression of microglia proliferation in infected *Ccr2*-KO and *Cx3cr1*-KO may be involved in the prevention of hippocampal neurodegeneration.

To assess if CCR2 and CX3CR1 also could be potential targets for therapy upon viral encephalitis-induced seizures and epilepsy, we investigated the impact of CCR2 and CX3CR1 on the development of seizures after TMEV infection. Surprisingly, we did not observe any significant reduction in seizure development upon *Ccr2* or *Cx3cr1* knock down except for a moderate decrease in seizure severity in the *Ccr2*-KO mice. Potential caveats to the interpretation of the present seizure data are the lack of continuous video-EEG monitoring and the restriction of seizure analyses to the day cycle, although the incidence of early seizures that we observed in B6-WT mice (67%) was quite similar to the 75% reported with continuous video-EEG monitoring (37).

Overall, the present data indicate that accumulation of myeloid cells in the CNS or hippocampus via infiltration of monocytes from periphery is not required for seizure development. Thus, it seems that, in contrast to several previous publications pointing toward monocytes being responsible for seizure development (14, 15, 21) our data with KO mice targeting monocytes suggest that monocytes alone are not responsible for the development of seizures during viral encephalitis. However, it must be mentioned that knockout of *Ccr2* still led to a significant decrease in seizure intensity. This observation suggests that monocytes could be involved in exacerbating the pathology during viral encephalitis-induced seizures. Thus, our data indicate that targeting the inflammation during viral encephalitis-induced brain pathology is a better strategy than targeting only specific cells, such as infiltrating monocytes.

The role of microglia activation in seizure development in the TMEV model is less clear. Previous studies with minocycline seemed to suggest that microglial activation contributes to seizures in the TMEV model (38, 39). However, the tetracycline antibiotic minocycline is not a selective inhibitor of microglial activation but exerts effects on multiple cellular targets involved in neuroinflammation, such as suppression of monocyte/macrophage activation and decreased infiltration of monocytes, T cells, and neutrophils into the CNS (40). In the present experiments, the lack of the fractalkine receptor CX3CR1, which is critical in microglia activation (5), was not associated with any reduction in the incidence or frequency of early (encephalitis-associated) seizures in the TMEV model. However, this does not exclude

a critical role for microglia in the development of epilepsy in this model.

Neuroinflammation with monocyte infiltration and microglial activation, as observed in rodent models of TLE, is also a frequently reported finding in patients with TLE (41–43). Thus, counteracting such inflammatory processes is considered a potential strategy for preventing or modifying epilepsy in patients at risk (2, 3, 44–47). For this strategy, it is imperative to better understand the complex crosstalk between microglia and other CNS-resident cells and infiltrating peripheral monocytes. Importantly, the delayed invasion of peripheral monocytes following brain insults provides a window of opportunity for treatment strategies aimed at preventing peripheral immune cells from entering the brain. CCR2 antagonists are efficacious after traumatic brain injury (47) and have entered clinical trials for the treatment of neuropathic pain (48). Fractalkine/CX3CR1 signaling is increased in microglia and modulates GABAergic currents in human epileptic brain (49). CX3CR1 is also involved during neuropathic pain (50), and the first CX3CR1 antagonists have recently been described (51, 52). One of these CX3CR1 antagonists has been reported to attenuate disease in a chronic-relapsing rat model for multiple sclerosis (52). The present data indicate that both CCR2 and CX3CR1 antagonists might be promising candidates for preventing the hippocampal damage after epileptogenic brain insults in response to viral encephalitis.

Materials and Methods

Animals and Tamoxifen Treatment. JAX C57BL/6J (B6) WT mice were purchased from Charles River Laboratories. According to a cooperative agreement between Charles River Laboratories and The Jackson Laboratory, the JAX C57BL/6J mouse strain bred by Charles River Laboratories in Europe is genetically equivalent to that bred by The Jackson Laboratory in the United States. *Ccr2*-KO mice (15, 53) and *Cx3cr1*-KO mice (54) were bred in-house. *Cx3cr1-cre*$^{ER+/-}$*tdTomato*$^{St/Wt}$ mice were bred at TWINCORE, Centre for Experimental and Clinical Infection Research, Hannover, Germany. All three mouse lines were generated on a JAX C57BL/6J background. To induce cre^{ER} activity, animals were treated s.c. after weaning with 4 mg of tamoxifen (Sigma) two times with a 48-h interval between treatments. To eliminate monocyte targeting, experiments were performed 6–8 wk after tamoxifen treatment. All mice were housed in groups under standardized conditions, with a 12-h/12-h day–night cycle, 50–60% humidity, 22–24 °C temperature, ad libitum tap water, and standard rodent diet (Altromin 1324 standard diet; Altromin International). The diet is produced by the vendor under strict quality control and regular analyses, including microbiology. Environmental enrichment was ensured by group houses and nesting material. Mice were randomly assigned to experimental groups (control vs. virus infection and postinfection groups). Following arrival, mice were allowed to acclimatize for at least 1 wk. All animal experiments were conducted in compliance with the German Animal Welfare Law and were approved by the institutional review board (ethics committee) and authorized by the local government (permission number 33.9-42502-04-11/0516; Niedersächsisches Landesamt für Verbraucherschutz und Lebensmittelsicherheit).

Infection. Mice were infected using the DA strain of TMEV as published previously (15, 55, 56). Briefly, mice were deeply anesthetized by isofluorane inhalation and, using a free-hand method of infection, were injected with either 20 μL TMEV solution (2.44×10^7 pfu) or a mock solution into the left parietal cortex. The dose of TMEV was based on previous experiments of our group in B6 mice to ensure a high incidence (>50%) of early seizures in this mouse strain (55). In most experiments, mice were killed 7 dpi (following seizure monitoring), because experiments with B6-WT mice in which myeloid cells, neuroinflammation, and neurodegeneration were compared at 2 and 7 dpi indicated that both neuroinflammation and neurodegeneration were most marked at 7 dpi.

Seizure Surveillance. To assess the development of acute seizures, mice were monitored twice daily for 1 h in the morning (between 9 and 12 AM) and 1 h in the afternoon (between 1 and 4 PM), with at least a 3-h interval between the two recording sessions. Care was taken to avoid any group differences in recording periods by randomly assigning animals to the recording sessions. Recording was performed by experienced researchers, and the choice of recording periods was based on previous experiments with video-EEG monitoring of acute seizures in this model [for more details see Bröer et al. (56)]. All flow cytometric and histological data shown in this study are from all animals infected with TMEV, not only from the animals infected with TMEV that presented with seizures.

Perfusion. On day 2 or 7 postinfection animals were deeply anesthetized with chloral hydrate i.p. and transcardially perfused with PBS followed by 4% paraformaldehyde. Brains were removed and left in 4% formaldehyde overnight before being cut and embedded in paraffin. Animals that were used for flow cytometric analysis were perfused with 4 °C PBS only. Brains were harvested and stored in 4 °C PBS until being further processed. EDTA-blood for flow cytometry was sampled before the start of perfusion analysis and was stored at 4 °C.

Histology and Immunohistochemistry. To assess inflammation and neurodegeneration, paraffin slides (2 μm) were stained with H&E or immunohistochemistry and analyzed as published recently (15, 25, 57). Histological analyses were focused on the dorsal hippocampus [at -2.06 ± 0.26 mm from bregma (mean ± SD; $n = 49$); section levels were determined by the stereotaxic mouse brain atlas of Paxinos and Franklin (58)], as this brain structure is mainly damaged due to a hippocampal tropism of TMEV and is also associated with the development of seizures and epilepsy. Section levels did not differ among groups. Neurodegeneration was assessed using NeuN immunostained slides (Merck Millipore) and was scored semiquantitatively [for details see Waltl et al. (15) and Polascheck et al. (59)]. Also, FJC staining was performed to visualize the presence of degenerating neurons (15, 60). Viral antigen labeling for TMEV in brain sections was performed via immunohistochemistry, using a polyclonal rabbit anti-TMEV capsid protein VP1-specific antibody (61).

For characterization of inflammatory processes, slides were stained using H&E and anti–Mac-3 (Bio-Rad) and were analyzed semiquantitatively (51). For quantification of myeloid cells, slides were stained using anti–Iba-1 (Abcam), and cells were counted manually. Cell proliferation was quantified by double staining slides using anti–Iba-1 (Wako) and anti-Ki67 (BD Pharmingen), and cells were counted manually in the ipsilateral hippocampus. All analyses were performed by two experienced researchers blinded to the experimental groups, and data of both researchers were averaged.

Immune Cell Isolation and Flow Cytometry. Immune cells were isolated from whole-brain homogenates as recently described (15). Briefly, brain tissue was processed using the neural tissue dissociation kit (Miltenyi Biotec) in accordance with the manufacturer's specifications. Afterward, cells were separated using a discontinuous Percoll density gradient (30–37–70% Percoll layers), which results in the enrichment of all immune cell types and removes a lot of myelin, which is auto-fluorescent. Following density gradient centrifugation, immune cells were washed and stained for 30 min at 4 °C using the following antibodies: CD11b APC-Cy7 (BD Biosciences), CD45.2 Pacific blue, CD86 PE-Cy5, and CD206 PE-Cy7 (BioLegend). Respective isotype control antibodies or unstained samples were used to determine positive populations. Myelin debris and dead cells were excluded by FSC/SSC gating, and singlet populations were analyzed.

For flow cytometric analyses of blood samples, EDTA-blood was stained at 4 °C for 15 min with the following antibodies: B220 Pacific Blue, CD3 AF700, CSF-1R BV605 (BioLegend), and CD11b APC-Cy7 (BD Biosciences). For more details see Waltl et al. (15).

Flow cytometry was performed using an LSRII flow cytometer (BD Biosciences), and data were analyzed using FlowJo software (Tree Star).

Statistics. GraphPad Prism Version 7 was used for all statistical analyses. Depending on the distribution of the data, either parametric or nonparametric statistical tests were applied. For comparisons of two groups, either a Student's *t* test or a Mann–Whitney *U* test was used; for groups larger than two an ANOVA *F* test, followed by a post hoc Dunnett's test or a Kruskal–Wallis test and a Dunn's post hoc test were performed. For comparison of different genotypes and treatments (sham vs. infection) and their interaction, data were analyzed by two-way ANOVA, followed by appropriate post hoc tests. Seizure frequencies were compared using Fisher's exact test. $P \leq 0.05$ was considered significant.

ACKNOWLEDGMENTS. We thank Robert S. Fujinami (Department of Pathology, University of Utah School of Medicine) for providing the DA strain of TMEV; Reinhold Förster (Department of Immunology, Hannover Medical School) for providing breeding pairs of Cx3cr1-KO mice; Sven Wehner (Department of Surgery, University of Bonn) for providing breeding pairs of

Ccr2-KO mice; and Julia Domdey, Petra Grünig, Claudia Herrmann, Katharina Lange, Christiane Namneck, Kerstin Schöne, Caroline Schütz, Danuta Waschke, Edith Kaczmarek, Michael Weissing, and Muneeb Anjum for skillful technical assistance. The study was supported by the Niedersachsen-Research Network on Neuroinfectiology of the Ministry of Science and Culture of Lower Saxony (W.L. and U.K.) and the Helmholtz Zukunftsthema Immunology and Inflammation (U.K.). C.K. was supported by the Studienstiftung des Deutschen Volkes e.V. C.C. was supported by a bilateral project of the German Centre for Neurodegenerative Diseases and the Helmholtz Centre for Infection Research (U.K.).

1. Klein P, et al. (2018) Commonalities in epileptogenic processes from different acute brain insults: Do they translate? *Epilepsia* 59:37–66.
2. Vezzani A, Lang B, Aronica E (2015) Immunity and inflammation in epilepsy. *Cold Spring Harb Perspect Med* 6:a022699.
3. Vezzani A, et al. (2016) Infections, inflammation and epilepsy. *Acta Neuropathol* 131: 211–234.
4. Prinz M, Priller J (2017) The role of peripheral immune cells in the CNS in steady state and disease. *Nat Neurosci* 20:136–144.
5. Ransohoff RM, Cardona AE (2010) The myeloid cells of the central nervous system parenchyma. *Nature* 468:253–262.
6. Prinz M, Priller J, Sisodia SS, Ransohoff RM (2011) Heterogeneity of CNS myeloid cells and their roles in neurodegeneration. *Nat Neurosci* 14:1227–1235.
7. Getts DR, et al. (2008) Ly6c+ "inflammatory monocytes" are microglial precursors recruited in a pathogenic manner in West Nile virus encephalitis. *J Exp Med* 205: 2319–2337.
8. Howe CL, LaFrance-Corey RG, Goddery EN, Johnson RK, Mirchia K (2017) Neuronal CCL2 expression drives inflammatory monocyte infiltration into the brain during acute virus infection. *J Neuroinflammation* 14:238.
9. Prinz M, Priller J (2010) Tickets to the brain: Role of CCR2 and CX3CR1 in myeloid cell entry in the CNS. *J Neuroimmunol* 224:80–84.
10. Chu HX, et al. (2014) Role of CCR2 in inflammatory conditions of the central nervous system. *J Cereb Blood Flow Metab* 34:1425–1429.
11. Varvel NH, et al. (2016) Infiltrating monocytes promote brain inflammation and exacerbate neuronal damage after status epilepticus. *Proc Natl Acad Sci USA* 113: E5665–E5674.
12. Howe CL, et al. (2012) Hippocampal protection in mice with an attenuated inflammatory monocyte response to acute CNS picornavirus infection. *Sci Rep* 2:545.
13. Howe CL, Lafrance-Corey RG, Sundsbak RS, Lafrance SJ (2012) Inflammatory monocytes damage the hippocampus during acute picornavirus infection of the brain. *J Neuroinflammation* 9:50.
14. Cusick MF, Libbey JE, Patel DC, Doty DJ, Fujinami RS (2013) Infiltrating macrophages are key to the development of seizures following virus infection. *J Virol* 87: 1849–1860.
15. Waltl I, et al. (2018) Macrophage depletion by liposome-encapsulated clodronate suppresses seizures but not hippocampal damage after acute viral encephalitis. *Neurobiol Dis* 110:192–205.
16. Bennett JL, et al. (2007) CCR2 regulates development of Theiler's murine encephalomyelitis virus-induced demyelinating disease. *Viral Immunol* 20:19–33.
17. Goldmann T, et al. (2013) A new type of microglia gene targeting shows TAK1 to be pivotal in CNS autoimmune inflammation. *Nat Neurosci* 16:1618–1626.
18. Goldmann T, et al. (2016) Origin, fate and dynamics of macrophages at central nervous system interfaces. *Nat Immunol* 17:797–805.
19. Tsou CL, et al. (2007) Critical roles for CCR2 and MCP-3 in monocyte mobilization from bone marrow and recruitment to inflammatory sites. *J Clin Invest* 117:902–909.
20. Landsman L, et al. (2009) CX3CR1 is required for monocyte homeostasis and atherogenesis by promoting cell survival. *Blood* 113:963–972.
21. DePaula-Silva AB, Hanak TJ, Libbey JE, Fujinami RS (2017) Theiler's murine encephalomyelitis virus infection of SJL/J and C57BL/6J mice: Models for multiple sclerosis and epilepsy. *J Neuroimmunol* 308:30–42.
22. Greter M, Lelios I, Croxford AL (2015) Microglia versus myeloid cell nomenclature during brain inflammation. *Front Immunol* 6:249.
23. Prinz M, et al. (2008) Distinct and nonredundant in vivo functions of IFNAR on myeloid cells limit autoimmunity in the central nervous system. *Immunity* 28:675–686.
24. Rock RB, et al. (2004) Role of microglia in central nervous system infections. *Clin Microbiol Rev* 17:942–964.
25. Loewen JL, Barker-Haliski ML, Dahle EJ, White HS, Wilcox KS (2016) Neuronal injury, gliosis, and glial proliferation in two models of temporal lobe epilepsy. *J Neuropathol Exp Neurol* 75:366–378.
26. Ajami B, Bennett JL, Krieger C, Tetzlaff W, Rossi FM (2007) Local self-renewal can sustain CNS microglia maintenance and function throughout adult life. *Nat Neurosci* 10:1538–1543.
27. Yamasaki R, et al. (2014) Differential roles of microglia and monocytes in the inflamed central nervous system. *J Exp Med* 211:1533–1549.
28. Galea I, et al. (2005) Mannose receptor expression specifically reveals perivascular macrophages in normal, injured, and diseased mouse brain. *Glia* 49:375–384.
29. Schmued LC, Stowers CC, Scallet AC, Xu L (2005) Fluoro-Jade C results in ultra high resolution and contrast labeling of degenerating neurons. *Brain Res* 1035:24–31.
30. Racine RJ (1972) Modification of seizure activity by electrical stimulation. II. Motor seizure. *Electroencephalogr Clin Neurophysiol* 32:281–294.
31. Buenz EJ, et al. (2009) Apoptosis of hippocampal pyramidal neurons is virus independent in a mouse model of acute neurovirulent picornavirus infection. *Am J Pathol* 175:668–684.
32. Kirkman NJ, Libbey JE, Wilcox KS, White HS, Fujinami RS (2010) Innate but not adaptive immune responses contribute to behavioral seizures following viral infection. *Epilepsia* 51:454–464.
33. Howe CL, et al. (2016) Neuroprotection mediated by inhibition of calpain during acute viral encephalitis. *Sci Rep* 6:28699.
34. Jafari M, et al. (2012) Impact of Theiler's virus infection on hippocampal neuronal progenitor cells: Differential effects in two mouse strains. *Neuropathol Appl Neurobiol* 38:647–664.
35. Libbey JE, Fujinami RS (2011) Neurotropic viral infections leading to epilepsy: Focus on Theiler's murine encephalomyelitis virus. *Future Virol* 6:1339–1350.
36. Brandt C, Potschka H, Löscher W, Ebert U (2003) N-methyl-D-aspartate receptor blockade after status epilepticus protects against limbic brain damage but not against epilepsy in the kainate model of temporal lobe epilepsy. *Neuroscience* 118:727–740.
37. Stewart KA, Wilcox KS, Fujinami RS, White HS (2010) Development of postinfection epilepsy after Theiler's virus infection of C57BL/6 mice. *J Neuropathol Exp Neurol* 69: 1210–1219.
38. Libbey JE, Kennett NJ, Wilcox KS, White HS, Fujinami RS (2011) Interleukin-6, produced by resident cells of the central nervous system and infiltrating cells, contributes to the development of seizures following viral infection. *J Virol* 85:6913–6922.
39. Barker-Haliski ML, et al. (2016) Acute treatment with minocycline, but not valproic acid, improves long-term behavioral outcomes in the Theiler's virus model of temporal lobe epilepsy. *Epilepsia* 57:1958–1967.
40. Möller T, et al. (2016) Critical data-based re-evaluation of minocycline as a putative specific microglia inhibitor. *Glia* 64:1788–1794.
41. Ravizza T, et al. (2008) Innate and adaptive immunity during epileptogenesis and spontaneous seizures: Evidence from experimental models and human temporal lobe epilepsy. *Neurobiol Dis* 29:142–160.
42. Zattoni M, et al. (2011) Brain infiltration of leukocytes contributes to the pathophysiology of temporal lobe epilepsy. *J Neurosci* 31:4037–4050.
43. Lu JQ, Steve TA, Wheatley M, Gross DW (2017) Immune cell infiltrates in hippocampal sclerosis: Correlation with neuronal loss. *J Neuropathol Exp Neurol* 76:206–215.
44. Vezzani A, French J, Bartfai T, Baram TZ (2011) The role of inflammation in epilepsy. *Nat Rev Neurol* 7:31–40.
45. Varvel NH, Jiang J, Dingledine R (2015) Candidate drug targets for prevention or modification of epilepsy. *Annu Rev Pharmacol Toxicol* 55:229–247.
46. Aronica E, et al. (2017) Neuroinflammatory targets and treatments for epilepsy validated in experimental models. *Epilepsia* 58:27–38.
47. Morganti JM, et al. (2015) CCR2 antagonism alters brain macrophage polarization and ameliorates cognitive dysfunction induced by traumatic brain injury. *J Neurosci* 35:748–760.
48. Biber K, Möller T, Boddeke E, Prinz M (2016) Central nervous system myeloid cells as drug targets: Current status and translational challenges. *Nat Rev Drug Discov* 15: 110–124.
49. Roseti C, et al. (2013) Fractalkine/CX3CL1 modulates GABAA currents in human temporal lobe epilepsy. *Epilepsia* 54:1834–1844.
50. Clark AK, Malcangio M (2014) Fractalkine/CX3CR1 signaling during neuropathic pain. *Front Cell Neurosci* 8:121.
51. Karlström S, et al. (2013) Substituted 7-amino-5-thio-thiazolo[4,5-d]pyrimidines as potent and selective antagonists of the fractalkine receptor (CX3CR1). *J Med Chem* 56:3177–3190.
52. Ridderstad Wollberg A, et al. (2014) Pharmacological inhibition of the chemokine receptor CX3CR1 attenuates disease in a chronic-relapsing rat model for multiple sclerosis. *Proc Natl Acad Sci USA* 111:5409–5414.
53. Kuziel WA, et al. (1997) Severe reduction in leukocyte adhesion and monocyte extravasation in mice deficient in CC chemokine receptor 2. *Proc Natl Acad Sci USA* 94: 12053–12058.
54. Jung S, et al. (2000) Analysis of fractalkine receptor CX(3)CR1 function by targeted deletion and green fluorescent protein reporter gene insertion. *Mol Cell Biol* 20: 4106–4114.
55. Bröer S, et al. (2016) Brain inflammation, neurodegeneration and seizure development following picornavirus infection markedly differ among virus and mouse strains and substrains. *Exp Neurol* 279:57–74.
56. Bröer S, et al. (2017) Viral mouse models of multiple sclerosis and epilepsy: Marked differences in neuropathogenesis following infection with two naturally occurring variants of Theiler's virus BeAn strain. *Neurobiol Dis* 99:121–132.
57. Gudi V, et al. (2009) Regional differences between grey and white matter in cuprizone induced demyelination. *Brain Res* 1283:127–138.
58. Paxinos G, Franklin KBJ (2012) *The Mouse Brain in Stereotaxic Coordinates* (Academic, New York), 4th Ed.
59. Polascheck N, Bankstahl M, Löscher W (2010) The COX-2 inhibitor parecoxib is neuroprotective but not antiepileptogenic in the pilocarpine model of temporal lobe epilepsy. *Exp Neurol* 224:219–233.
60. Gröticke I, Hoffmann K, Löscher W (2008) Behavioral alterations in a mouse model of temporal lobe epilepsy induced by intrahippocampal injection of kainate. *Exp Neurol* 213:71–83.
61. Kummerfeld M, Meens J, Haas L, Baumgärtner W, Beineke A (2009) Generation and characterization of a polyclonal antibody for the detection of Theiler's murine encephalomyelitis virus by light and electron microscopy. *J Virol Methods* 160:185–188.